

THE ANALYSIS OF FIBER SENSOR OF TEMPERATURE FIELD DISTURBANCE BY HUMAN BODY PART ACCESS

Filip DVORAK¹, Jan MASCHKE², Cestmir VLCEK²

¹Department of radar technology, Faculty of Military Technology, University of Defence, Kounicova 65, 662 10 Brno, Czech Republic

²Department of electrical engineering, Faculty of Military Technology, University of Defence, Kounicova 65, 662 10 Brno, Czech Republic

flip.dvorak@unob.cz, jan.maschke@email.cz, cestmir.vlcek@unob.cz

Abstract. The principle of this sensor function is based on polarization maintaining fiber (PMF) sensitivity during excitation of both two polarization modes. This excitation is caused by temperature change, when absorbing thermal radiation. This mechanism is used for detection of temperature field disturbance as an indicator. In the case described below, attention was devoted to temperature field disturbance on the part of the human body. Thus, this sensor system could be used for protection of some entity. The aim of this study was to determine the sensitivity of PMF to radiating heat, the space configuration and time response.

Keywords

Fiber sensor, PMF, temperature field disturbance.

1. Introduction

Polarization maintaining fibers (PMF) work on the basis of creating the mechanical strain that causes artificial birefringence. Typical fiber applications include cases, where state polarization maintenance along the light propagation through the fiber is required, and where the excitation of one polarization axis occurs. One effective way of creating birefringence is arranging structures with different thermal expansion into a fiber cladding. At an excitation of both polarization axes, when the light propagates through the fiber, the phase shift happens between these axes. The phase shift is dependent on temperature and therefore is dependent on incident thermal radiation and is dependent on change of the polarization state along the fiber as well. This phase shift can be evaluated by polarizer (analyzer). Previous experiments [1], [2] showed, that the most suitable fiber, from the sensitivity point of view,

is PANDA type fiber. The results achieved suggested to apply such sensor in cases, where the temperature field is disturbed by human body proximity, i.e. in the range of specific temperatures. Suitable application could be, for example, property protection against illegal manipulation and therefore some requirements for the sensor sensitivity, system configuration and time response were established.

2. Model of Fiber Thermal Segment Exposition

Setup of experimental workplace is shown in Fig. 1. The thermal body is simulated by a plastic basin with warm water. This arrangement enables changes in the test water temperature, basin bottom distance from the fiber and the number of exposed fiber segments. In the case more fiber segments are exposed, and two plastic basins are used.

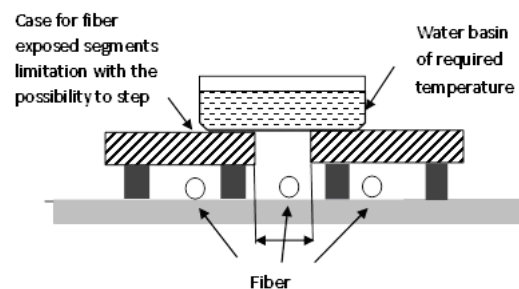


Fig. 1: The arrangement of fiber sensor model.

2.1. Model Description

The model of fiber sensor for detection of temperature field disturbance caused by human body part was set to

simulate realistic conditions and also to define analysis and subsequent conditions. Thermal exposition was realized by a body of defined temperature and placed a 6 cm basin bottom distance from the exposed fiber segment. For shorter distances (to 13 cm) the response of PMF has linear characteristic and for longer distances it has non-linear characteristic. The range of temperatures between 35 °C and 45 °C was selected, i.e. corresponding to the normal body temperature of about 37 °C. Then a sufficiently wide range of dependencies around this temperature were selected. Three mechanisms need to be considered for temperature transfer to the fiber: the thermal radiation of the body, heat transfer, and the absorption of heat by the fiber.

1) Mechanism of Thermal Radiation

Thermal power P radiated by the body can be described by the radiation law [3]:

$$P = \sigma \varepsilon S T^4 = K_R T^4, \quad (1)$$

where σ is Stefan-Boltzmann constant, ε is emissivity (characterizing circumference), S is surface and T is the absolute temperature.

Considering the parameters of the applied body were constant during the experiments, they could be included to the constant K_R in Eq. (1). With regards to the relative small range of temperatures interested, we could consider linear dependence of power upon temperature. Graph of the fourth power in relative units ($T^4/10^8$) for temperatures in a range from 308 K to 318 K (corresponding to 35 °C - 45 °C) is presented in Fig. 2. This relation can be assumed linear and thus the radiated power can be assumed as proportional to the absolute temperature. The radiated power shown in Fig. 2 is relative to the radiated power with temperature 298 K (25 °C). Variation of linearity is less than 1 %.

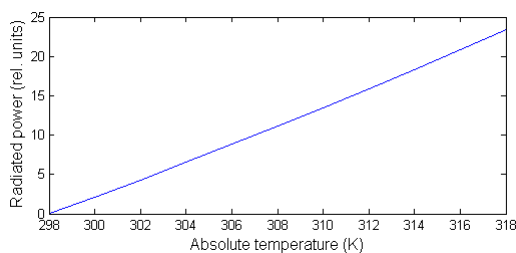


Fig. 2: Radiated power (norm function $P = 10^{-8} \cdot T^4$ versus temperature.

2) Mechanism of Heat Transfer

Transferred heat Q_T from a body of temperature T_e on a body of temperature T was calculated as follows:

$$Q_T = \lambda_T \frac{S}{\Delta l} (\Delta T_e - \Delta T) t = K_T (\Delta T_e - \Delta T) t, \quad (2)$$

where λ_T is a coefficient of thermal conductivity, Δl is the the heat source (basin bottom) distance from the fiber segment, S is the surface area, ΔT_e is temperature difference between the source and ambient temperature, ΔT is the temperature difference between the body and ambient temperature and t is time.

As the phase shift is calculated with respect to the change of temperature, all temperatures are relative to the initial temperature of the fiber, i.e. to the difference between given and the ambient temperature Δ .

As the transfer of heat depends on the difference between the temperatures, we substituted the difference of absolute temperatures T by the difference of temperatures $\Delta\vartheta$ in °C, in which the temperature of the applied body was measured and we obtain formula:

$$Q_T = K_T (\Delta\vartheta_e - \Delta\vartheta) t. \quad (3)$$

3) Heat Absorption

Heat absorbed by the body Q_A was calculated as [3]:

$$Q_A = c_m m \Delta\vartheta, \quad (4)$$

where m is the mass of the absorbing body, c_m is the specific heat capacity. Because m is proportional to the length l , the following formula applies:

$$m = k_m l, \quad (5)$$

where k_m is constant including the profile and the specific mass of the fiber. Equation (5) can be put into Eq. (4) as:

$$Q_A = c_m k_m l \Delta\vartheta = K_A l \Delta\vartheta, \quad (6)$$

where K_A covers the dependence of specific capacity and proportion parameters, relative to the fiber profile and the specific mass. The following formula applies for differentials of transfer functions Eq. (2) and absorbing Eq. (6):

$$dQ_T = K_T (\Delta\vartheta_e - \Delta\vartheta) dt, \quad (7)$$

$$dQ_A = K_A l d\Delta\vartheta. \quad (8)$$

If we suppose that all transferred heat is absorbed, the following formula applies:

$$K_A l d\Delta\vartheta = K_T (\Delta\vartheta_e - \Delta\vartheta) dt. \tag{9}$$

Then we obtain a simple differential equation:

$$\frac{d\Delta\vartheta}{\Delta\vartheta - \Delta\vartheta_e} = \frac{K_T}{K_A l} dt. \tag{10}$$

Solution of the equation is in the following form:

$$\Delta\vartheta = \Delta\vartheta_e \left[1 - \exp\left(-\frac{K_T}{K_A l} t\right) \right]. \tag{11}$$

If we suppose that the phase shift changes in the given and relatively small range of temperatures of 35 °C to 45 °C proportionally with the temperature, then change of the phase copies approximately Eq. (11). The value of optical intensity behind the polarizer with turning 45° was proportional to the cosine of the phase shift.

4) Phase Response to the Thermal Exposition

Suppose that the phase shift is linearly proportional to temperature, during a relatively small range of temperatures. As proven by previous measurements, phase shift can be written as follows:

$$\delta = K_\pi \Delta\vartheta, \tag{12}$$

where K_π is proportional constant (rad/°C) and is defined from the experimentally obtained dependencies.

By substituting $\Delta\vartheta$ from Eq. (12) to Eq. (11), we obtain:

$$\delta = \delta_\infty \left(1 - \exp\left(-\frac{K_T}{K_A l} t\right) \right). \tag{13}$$

Here $\delta_\infty = K_\pi \Delta\vartheta$ is the phase shift in infinity. To create a common model, norm value of Eq. (13) should be reflected as:

$$\frac{\delta}{\delta_\infty} = \left(1 - \exp\left(-\frac{K_T}{K_A l} t\right) \right). \tag{14}$$

2.2. The Output Signal of the Sensor

It is clear from Eq. (14) that the phase shift changes exponentially during time depending on settings, characterized by the fiber length, and constants representing radiation, transport, and absorption of the heat.

In the designed sensor system we assume a relatively short fiber segment, in order of units or maximum of tens of meters, according to the coherence of the optical source. In this case we assumed also propagation of the eigenmodes without any significant mutual coupling. The phase shift change at the end of the fiber was analyzed by the polarizer (analyzer) set about 45° towards the polarization axes, where the maximum intensity response to the phase shift changes was achieved. In an ideal case of circular polarization at the input of the fiber, the intensity behind the polarizer changed from maximum to the zero value. In the case of imperfect circular polarization, the intensity in the output decreased to a minimum, however not to zero. A similar effect can happen in case the coherence between both polarization components is disturbed. The phase shift evaluation is provided in Fig. 3.

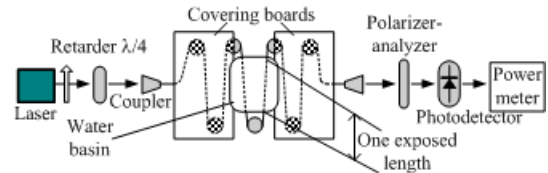


Fig. 3: The set of sensor for measurement.

It is possible to show from Fig. 3 that we measured Stokes component S_2 in the polarizer output. For this arrangement Stokes components S_1 and S_{-1} corresponded to the polarization axes of PMF (see Fig. 4).

For the excitation of fiber, corresponding to a point on the equator of observable Poincare sphere [4], S_2 could be expressed as follows:

$$S_2 = S_0 \cos \delta. \tag{15}$$

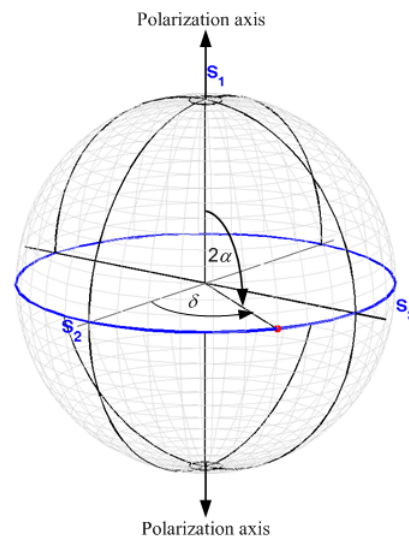


Fig. 4: The set of polarization axes PMF towards polarizer (analyzer) oriented in S_2 .

This equation is valid for fully polarized radiation. In the case of partially polarized radiation, an unpolarized component can occur at the expense of polarized one during the process of propagation through the fiber. Then, the intensity of the polarized component can be expressed as:

$$I = S_2 = pS_0 \cos \delta, \tag{16}$$

where I is generally measured intensity on the output of the polarizer, and p is the degree of polarization.

Insufficiently modulated output signal could not be only a result of lower polarization degree, but also of the unequal excitation of polarization axes, e.g. as in the case of laser diode with noncircular beam profile. The resultant intensity, measured in the output of the polarizer includes, in general, constant and variable parts. For a linear variation of the phase shift, the variable part of the resultant intensity should change harmonically. In the case the phase shift depends on the time Eq. (14) normed output intensity could be expressed as:

$$I = 1 - A + A \cos \left[\delta_\infty \left(1 - \exp \left(-\frac{K_T}{K_A l} t \right) \right) \right], \tag{17}$$

where A is amplitude of variable intensity part.

Time behavior of phase shift variation and its corresponding intensity at the polarizer output is presented in Fig. 5. Curves are valid for normed value of the phase $\delta/\delta_e = 1$ in Eq. (13) and $A = 0.4$ for Eq. (17). Evaluation of the polarization degree is not quite definite. Fixed parts of the output signal could be created by both the unpolarized radiation - as a result of decreasing the degree of coherence between the polarization components during their propagation along the fiber and the unequal excitation of polarization components caused by noncircular laser beam profile. For the examination of this phenomenon, the term polarization efficiency p_{ef} was introduced, expressing proportion of variable and constant intensity components.

$$p_{ef} = \frac{A}{1 - A}, \tag{18}$$

from this

$$A = \frac{p_{ef}}{1 + p_{ef}}, \tag{19}$$

we can write Eq. (17) as:

$$I = \frac{1}{1 + p_{ef}} + \frac{p_{ef}}{1 + p_{ef}} \cos \left[\delta_\infty \left(1 - \exp \left(-\frac{K_T}{K_A l} t \right) \right) \right]. \tag{20}$$

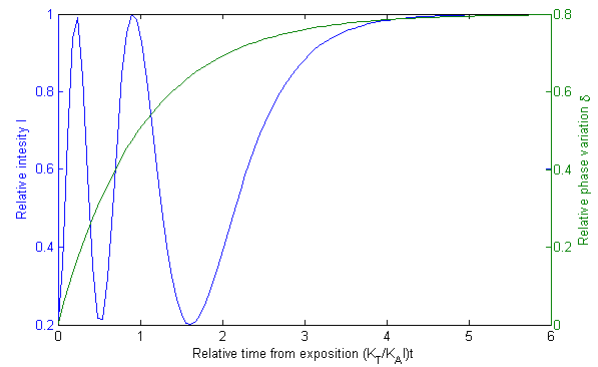


Fig. 5: Model behavior of normed value of the phase change and corresponding intensity.

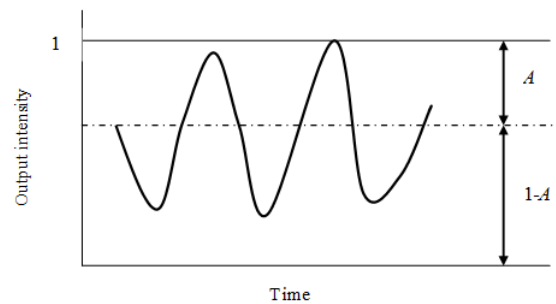


Fig. 6: Model behavior of output intensity.

Constant and variable components of output intensity for polarization efficiency from 0 to 1 are shown in Fig. 7.

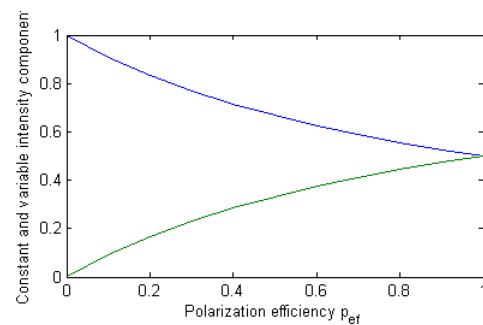


Fig. 7: Dependence of the constant and variable components of intensity on the polarizer output.

2.3. The Experimental Verification and Evaluation of the Time Response

1) Optical Fiber - PMF 633, Optical Source He-Ne and LD 633, the Same Length

A demonstration of the time response for this set of components is depicted in Fig. 8 and Fig. 9. Some difference in the output polarization is evident from these

graphs. The polarization efficiency and important values for its determination are in Tab. 1.

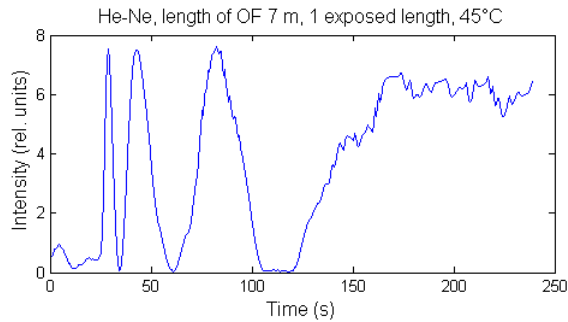


Fig. 8: Time dependence of the output intensity for excitation PMF by He-Ne laser.

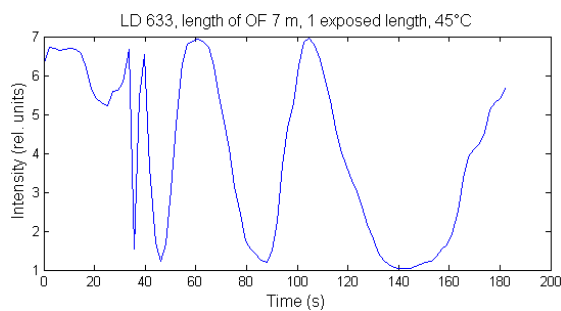


Fig. 9: Time dependence of the output intensity for excitation PMF by LD 633.

Tab. 1: Polarization efficiency for PMF 7 m of length, excited by He-Ne and LD633, exposition temperature 45 °C.

Optical source	LD 633	He-Ne
Maximum value	6.97	7.43
Minimum value	1.05	0.05
Peak-to-peak amplitude	5.92	7.38
Peak-to-peak amplitude/2	2.96	3.69
Mean value (peak-to-peak/2+min. value)	4.01	3.74
Polarization efficiency (peak-to-peak/2/mean value)	0.73	0.98

By comparing results in this table, the conclusion is as follows:

- Effect of coherence on the time response caused by thermal exposition.
- Insufficient circular polarization in the fiber input can be caused not only by a low degree of coherence, but also by a noncircular LD beam profile.
- From the practical realization point of view it is necessary to take into considerations the excitation by LD with regard to the compatibility of individual sensor components.

2.4. The Time Response to Thermal Exposition

The experimental test was conducted for the wavelength $\lambda = 633$ nm. For the excitation of PMF, the HL6312G semiconductor laser was used. Circular polarization was obtained behind the linear retarder $\lambda/4$. The total length of PMF was 7 m. In the measured time dependencies, some invariance occurs. This was caused by the fiber length and also partially by the input noncircular beam profile. With respect to the test character that focused, on the determination of phase shift variation, the separation into polarized and unpolarized parts was not important. One unit of the exposed length was the length of the temperature body (Fig. 3) that equaled to 0.27 m. To make it clearer in the following text, graphs, and tables, the segments were marked as first segment and second segment. The experiment was conducted as follows:

- Two exposed PMF segments with the same length as the exposed length, each with different position with respect to the total length of PMF, were exposed to the effect of external temperature body. Distances of first segment and second segment from the beginning of PMF were 2.91 m and 4.32 m respectively..
- In the first part of the test the second segment was exposed to the effect of external temperature body and after certain time interval the first segment was also exposed.
- In the second part of the test, both segments were exposed simultaneously.

To obtain the PMF response sufficiently the temperature of the external body was adjusted to 45 °C. Time dependencies of phase shift variation marked with a sample number are shown in Fig. 10. The sample period was 1.1 s. Adequate time constants were determined from these time dependencies. Some particular time constants are presented in Tab. 2.

To model the response of the temperature field disturbance sensor we determined specific constant characterizing the response to the unit of fiber length in this particular arrangement. If we assume time dependence of phase shift variation as in Eq. (14), then the time constant can be determined as 63 % of its maximum value as follows:

$$\frac{K_T}{K_{Al}} = \frac{1}{t_{63}}, \quad (21)$$

where t_{63} is time constant corresponding to 63 % of its maximum (steady) value.

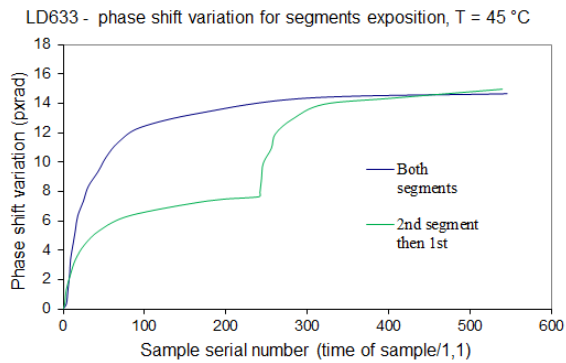


Fig. 10: Phase shift variation for segments exposition.

Tab. 2: Phase shifts and time constants evaluation.

Exposition procedure	2nd then 1st segment		Simultaneously
	1st	2nd	
Phase shift maximum value [rad]	7.45	7.4	14.6
63 % of max. value [rad]	4.7	4.7	9.2
ts [s]	33	33	46.2

The PMF response value and its sensor sensitivity are increasing with the increasing exposed length. This is clear from time dependences in Fig. 10 and from the obtained results in Tab. 2. On the other hand, the increased exposed length and, simultaneously exposed segments, increased time constant t_{63} more than the exposition of only one length. This could be also calculated from Eq. (21) where the dependence on the exposed length was determined. It can be deduced that for longer exposed length (simultaneously), the time constant will be increasing hugely with nonlinear characteristic and its speed will be decreasing. The resultant total response of PMF is almost identical for the two cases of gradually (second then first) exposed segments and simultaneously exposed segments.

3. Conclusion

Proposed sensor arrangement is the advantage for surveillance purposes covering wide area on condition the laser sources with the sufficient coherency are used. For significant exposed length there is the appropriate response. The option of adjusting the sensitivity by changing the exposed length is also advantageous. A fast sensor response was achieved by exposition of short segments simultaneously.

One disadvantage of the sensor is its sensitivity to other factors, e. g. mechanical vibration. This could be turned into the advantage, when, for example surveilling surrounding environment. Another disadvantage is the requirement of photonics components to

be a linear retarder and polarizer, compatible with the optical fiber sensor.

Future work will be aimed at the studying other effects factors impacting the sensor sensitivity from the laser source coherency and, radiating characteristic point of view. Then the effects of these external factors like mechanical vibrations will be studied. The main aim of our future work is to realize a compact sensor as an electronic evaluating system. This system will represent a particular optical receiver with digital signal convertor.

Acknowledgment

This work has been supported by Projects for the development of K217 and K207 Departments, Brno University of Defense – Modern electrical elements and systems.

References

- [1] DVORAK, F., J. MASCHKE and C. VLCEK. Utilization of birefringent fiber as sensor of temperature field disturbance. *Radioengineering*. 2009, vol. 18, no. 4, pp. 639–643. ISSN 1210-2512.
- [2] DVORAK, F., J. MASCHKE and C. VLCEK. Response analysis of thermal field disturbance sensor. In: *SPIE Security+Defence*. Prague: SPIE, 2011, pp. 501–508. ISBN 978-0819488138.
- [3] HALLIDAY, D., R. RESNICK and J. WALKER. *Fundamentals of physics*. Chichester: Wiley, 2007. ISBN 978-1-118-23072-5.
- [4] COLLETT, E. and B. SCHAEFER. Visualization and calculation of polarized light. I. The polarization ellipse, the Poincare sphere and the hybrid polarization sphere. *Applied optics*. 2008, vol. 47, no. 22, pp. 4009–4016. ISSN 1559-128X.
- [5] BORN M. and E. WOLF. *Principles of optics*. Cambridge: Cambridge University Press, 1999. ISBN 978-0-521-64222-4.
- [6] COLLETT, E. *Polarized light in fiber optics*. New Jersey: SPIE Press, 2003. ISBN 978-0819457615.

About Authors

Filip DVORAK was born in 1977. He received his M.Sc. degree from the Brno Military Academy in 2004 and Ph.D. degree in 2011. He is currently lecturer with the Department of Radar Technology,

Brno University of Defense. His work is focused on the modeling of fibers and optical components by means of matrix methods in the MATLAB environment and analysis of fiber sensors.

Jan MASCHKE was born in 1942. He received his M.Sc. degree in 1965 and Ph.D. degree in 1978. He was a teacher at the Technical school at Liptovský Mikuláš and at the Military Academy since 1968, and associate professor of the Department of electrical engineering since 1985. He retired in 2005. His research work focused on the problems of fiber optics and fiber sensors.

Cestmir VLCEK was born in 1946. He received his M.Sc. degree in 1969 and Ph.D. degree in 1980. He was a teacher at the Military Academy since 1969, associate professor since 1985, head of the Electrical Engineering and Electronics Department since 1997 and professor since 2000. His research work during the last years was aimed at problems of optoelectronic signals and systems, single mode fiber components modeling, atmospheric optical communication systems and analysis of sensors for military applications.